Temperature Compensation of Total Power Radiometers

David A. Thompson, Robert L. Rogers, *Senior Member, IEEE*, and John H. Davis, *Member, IEEE*

***Abstract*—This paper describes a new technique to compensate output variations of total power radiometers due to physical temperature changes of the instrument. This technique performs the correction without the addition of expensive microwave hardware required in Dicke switching or many other widely used methods. A characterization period, over which the input antenna temperature is known, indicates the appropriate output adjustment needed for a change in physical temperature of the radiometer. The method effectively corrects the output in an example radiometer system built with inexpensive commercially available parts. For a 30-K variation in physical temperature, the measured data shows an improvement from 60-K peak-to-peak error to 6.9 K with an average absolute error of 1.1 K.**

***Index Terms*—Microwave radiometer, microwave receiver, passive sensing, remote sensing, temperature compensation, total power radiometer.**

I. Introduction

A TOTAL power radiometer collects, amplifies, and detects electromagnetic radiation. Calibrating the instrument consists of finding parameters relating the received power to the temperature of a black body producing an equivalent amount of power. If the characteristics of the radiometer change after calibration, the parameters become invalid. Normal applications expose the instrument to physical temperature variations causing corresponding changes in the radiometer's uncorrected output. The temperature-compensation method uses the physical temperature of the entire receiver to adjust a set of coefficients, which compensate for both gain and receiver noise variations. A characterization period, over which the input antenna temperature is known, indicates the appropriate output adjustment needed for a change in physical temperature of the radiometer.

In this paper, we will refer to a two-point calibration in the sense commonly used with radiometers. In a two-point calibration, the receiver (radiometer) looks at known loads and utilizes their associated outputs to infer the relationship between the output voltage and antenna temperature. This calibration only corresponds to a single physical temperature of the receiver. In contrast, the temperature-compensation method's characterization relates the antenna temperature and the output voltage for a range of physical device temperatures. Once the radiometer output is characterized according to the physical temperature, calibration is no longer necessary since the output is compensated. In principle, this characterization should be valid as long as the physical configuration of the radiometer is maintained.

Historically, output variations have been handled by recalibrating periodically [1] or by using switched-type radiometers [2]–[13]. Constant recalibration gives less time for data collection, and switched radiometers have lower sensitivity, greater complexity, and higher cost compared to total power radiometers. Switching methods all require extra microwave hardware (low insertion-loss microwave switches, calibration loads, etc.). In contrast, the temperature-compensation method does not need these components. It is, therefore, less expensive to implement and suitable for applications where instrument cost is a major concern.

Many applications require radiometer systems in which only limited power is available. The temperature-compensation method offers reduced power consumption when compared to switching techniques by eliminating the significant power consumption of the microwave switches, such as latching circulators and p-i-n diode switches. Although a programmable microcontroller would be needed, a microcontroller requires far less power than the switches they replace. This method also eliminates the need for active temperature stabilization of the radiometer since the output variations due to changes in the physical temperature are corrected. Thus, power savings can be realized by avoiding active heating or cooling of the radiometer to maintain a constant temperature of the electronics.

Temperature compensation has been suggested by previous authors, but not fully implemented. Skou [14] suggests a method using the physical temperature to compensate for gain variations for an unbalanced Dicke-switched radiometer. However, this did not eliminate the need for a front-end Dicke switch. Al-Ansari *et al.* [15] used a temperature-correction scheme for a total power radiometer. However, only gain variations of the RF amplifiers are included and the method does not allow for fluctuations in uncorrected output data caused by receiver noise temperature changes.

II. Temperature Compensation of Calibration Parameters

Fig. 1 shows a block diagram of a total power radiometer. The power at the input to the square-law detector diode is

$$P = k\,(T_A + T_R)\,\mathrm{BG} \tag{1}$$

where k is the Boltzman's constant, T_A is the antenna temperature we wish to determine, T_R is the receiver noise, B is the

Manuscript received November 12, 2002; revised March 2, 2003.

D. A. Thompson is with the Aerospace Corporation, El Segundo, CA 90245-4691 USA.

R. L. Rogers is with the Applied Research Laboratories, The University of Texas at Austin, Austin, TX 78713-8029 USA.

J. H. Davis is with the Department of Electrical and Computer Engineering, The University of Texas at Austin, Austin, TX 78712 USA (e-mail: jhd@mail.utexas.edu).

Digital Object Identifier 10.1109/TMTT.2003.817679

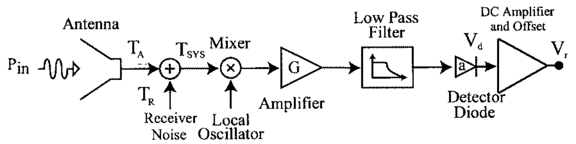

Fig. 1. Block diagram of total power radiometer.

bandwidth of the pre-detection filter, and G is the gain along the signal path. After detection, an amplification of α_r and offset of β_r condition the signal for data acquisition giving

$$V_r = \alpha_r V_d + \beta_r = \alpha_r a_r k\left(T_A + T_R\right)\mathrm{BG} + \beta_r \qquad (2)$$

where V_d is the diode output voltage and a_r is the sensitivity of the diode. As long as α_r, a_r, β_r, and BG remain constant, the output voltage depends only on the antenna temperature.

A calibration, defined by a slope m_c and offset b_c, maps the voltage V_r to a calibrated output of

$$T_a = m_c V_r + b_c = m_c \alpha_r a_r k\left(T_A + T_R\right)\mathrm{BG} + m_c\beta_r + b_c. \qquad (3)$$

If we require the calibrated output to be equal to the antenna temperature, the calibration coefficients take the following forms:

$$m_c = \frac{1}{\alpha_r a_r k\mathrm{BG}} \qquad (4)$$

$$b_c = -T_R - m_c\beta_r. \qquad (5)$$

A shift in physical temperature causes changes in the low-frequency op-amp circuitry (α_r, β_r) [14], diode sensitivity, gain, and system noise [16]. By tying all components to the same heat sink and assuming that the characteristics of any component is a single-valued function of the heat-sink temperature, the calibration coefficients are also single-valued functions of the physical temperature

$$m_c = m_c\left(T_{\mathrm{phy}}\right) \qquad (6)$$

$$b_c = b_c\left(T_{\mathrm{phy}}\right). \qquad (7)$$

One can expand these in a power series form to get

$$m_c = m_0 + m_1 T_{\mathrm{phy}} + m_2 T_{\mathrm{phy}}^2 + m_3 T_{\mathrm{phy}}^3 + \cdots \qquad (8)$$

$$b_c = b_0 + b_1 T_{\mathrm{phy}} + b_2 T_{\mathrm{phy}}^2 + b_3 T_{\mathrm{phy}}^3 + \cdots \qquad (9)$$

where $m_0, m_1, m_2, m_3, \ldots$ and $b_0, b_1, b_2, b_3, \ldots$ are constants to be determined. In practice, one only uses a few terms in (8) and (9) and determines the coefficients by using a characterization period as described in Section III.

III. Characterization

In order to determine the calibration coefficient constants of (8) and (9), we obtain data in a calibration period over which the dependence of the output of the radiometer on its physical temperature is characterized. During this time, one finds a set of the m's and b's defined above using a least squared error method. Outside of this characterization period, no further calibration is necessary. The output voltage from the radiometer and the results of the characterization determine the calibrated and corrected antenna temperature.

The procedure uses the un-calibrated radiometer output voltage, physical temperature, and known antenna temperature produced by a calibration load. Using (3), we can define an error at each sample in time i during the period as

$$\begin{aligned}\mathrm{error}_i &= T_{Ai} - m_c V_{Ai} - b_c \\ &= T_{Ai} - \left(m_0 + m_1 T_{\mathrm{phy}}\right) V_{ri} - \left(b_0 + b_1 T_{\mathrm{phy}} + b_2 T_{\mathrm{phy}}^2\right).\end{aligned} \qquad (10)$$

An approximation to (8) and (9) is used here with two terms in the slope and three in the offset, although more terms could have been used. We can now utilize the method of least squared errors over all samples in the characterization period to find the constants. Outside the characterization period, we find the antenna temperature using

$$T_a = \left(m_0 + m_1 T_{\mathrm{phy}}\right) V_r + \left(b_0 + b_1 T_{\mathrm{phy}} + b_2 T_{\mathrm{phy}}^2\right). \qquad (11)$$

To minimize the error in the predicted m's and b's, the characterization should use the largest expected range of both physical and antenna temperature in the data. The range of physical temperatures used for the characterization should be at least as great as the range of physical temperatures the radiometer is expected to experience in operation. In addition to the requirement to observe changes in the physical temperature of the radiometer, one must also observe changes in the temperature of the input load. Observing these temperatures along with the raw output voltage of the radiometer allows the m's and b's in (10) to be obtained by least squares fitting. Wider temperature ranges provide better values for the parameters. However, doing so will give multiple data points over a wide spread in antenna temperature for a given physical temperature. If one expects large differences in the temperatures entering the antenna, the nonlinearities of the amplifier or deviation of the detector from square law behavior could cause errors of the extent of the small-signal changes of interest.

IV. Radiometer and Calibration Load

We designed the radiometer to demonstrate the effectiveness of this method on a low-cost receiver. To meet this end, we did not include an RF amplifier between the antenna and mixer. This places great importance on compensating for temperature-dependent system (receiver) noise. The radiometer operated at 26 GHz, and its parts are listed in Table I. As shown in Fig. 1, signals were immediately down converted to baseband after the antenna. They then entered an inexpensive dual stage IF amplifier with approximately 65 dB of gain when averaged over a 1-GHz bandwidth and a 2-dB noise figure. With the 7.5-dB conversion loss of the mixer and its noise, the radiometer's total noise figure was significantly higher than the amplifiers' and was estimated from the random fluctuations on V_r and the estimated bandwidth (discussed below) to be approximately 9.5 dB.

To get an idea of how different components can affect the output signal of the radiometer, we measured the physical temperature dependence of the gain–bandwidth product of the amplifier–filter combination, amplifier noise temperature, and diode output voltage. The gain of the amplifier varied with

TABLE I
COMPONENTS USED IN THE TEMPERATURE-COMPENSATED RADIOMETER

Part	Description
Antenna	Millitech KA-band cassegrain reflector antenna with a 1 ft. diameter
Amplifier	Mini-Circuits ZKL-series amplifier package and RF board modified to accommodate two Hewlett-Packard INA-02170 50 Ω amplifier gain blocks
Mixer	Miteq DB0440LW1 with 7.5 dB conversion loss
Local Oscillator	Narda NKO-KF-26000 26 GHz DRO
Low Pass Filters	Lark Engineering LMC1000-3AA, 1 GHz 3dB cutoff frequency, ceramic, 3 section low pass filter
Diode	Herotek DT 1040 tunnel diode (backward diode) detector with nominal sensitivity of 800 mV/mW
Attenuators	JFW Industries, various values
Temperature Measurement	Analog Devices AD592AN precision IC temperature transducer

frequency, as well as temperature. Its gain began rolling off before the 1-GHz cutoff frequency of the low-pass filter. For this reason, it is necessary to measure the gain–bandwidth product BG defined as

$$\mathrm{BG} = \int_0^{f_c} G(f)\,df \tag{12}$$

where $G(f)$ is the frequency-dependent amplifier gain, and f_c is the cutoff frequency of the filter. We measured the frequency-dependent gain on a Hewlett-Packard 8752A network analyzer in 0.5 °C increments at physical temperatures between 7.5 °C–56.5 °C. We used (12) to get the gain–bandwidth product at each temperature.

A Hewlett-Packard 8970A noise-figure meter and 346B noise source measured the noise temperature in a 4-MHz bandwidth centered at 29 discrete frequencies between 100–500 MHz. The noise power output by the amplifier P_n over the low-pass filter's passband is

$$P_n = k\int_0^{f_c} G(f)\,T_{\mathrm{amp}}(f)\,df \tag{13}$$

where $T_{\mathrm{amp}}(f)$ is the amplifier's frequency-dependent noise temperature. We can define an effective noise temperature T_{eff} such that noise power out of the amplifier is

$$P_n = kT_{\mathrm{eff}}\mathrm{BG}. \tag{14}$$

Combining (13) and (14), the effective noise temperature is

$$T_{\mathrm{eff}} = \frac{\int_0^{f_c} G(f)\,T_{\mathrm{amp}}(f)\,df}{\mathrm{BG}}. \tag{15}$$

Note that this is T_{eff} at a particular physical temperature. This means that $G(f)$, $T_{\mathrm{amp}}(f)$, and BG must be measured at the same physical temperature. We did this in 1 °C increments from 10 °C to 53 °C.

The diode detecting a radiometer's signal sees a band of frequencies. To simulate this, we constructed a noise source from the amplifier with a terminator on the input. The noise source was held at a constant temperature. The amplifier output was filtered with the same low-pass filter used in the radiometer. The power was attenuated to a level of −28.7 dBm before detection. Measurements of the detector diode showed that systematic deviation from square law behavior was not measurable below −24 dBm of input power. The output voltage was given a known dc amplification and collected continuously using a National Instruments PCI-6023E data acquisition card and a computer as the diode's temperature was varied between 0 °C–45 °C.

In each case, straight lines with the following equations fit the data very well:

$$\mathrm{BG} = 3.35\times10^{15} - 1.79\times10^{13}\cdot T_{\mathrm{phy}} \tag{16}$$

$$T_{\mathrm{eff}} = 146 + 0.837\cdot T_{\mathrm{phy}} \tag{17}$$

$$V_d = -8.89\times10^{-4} - 4.82\times10^{-6}\cdot T_{\mathrm{phy}} \tag{18}$$

where BG is in hertz, T_{eff} is in kelvin, V_d is in volts, and T_{phy} is in Celsius. The standard deviation between the line and the gain–bandwidth product data is 4.73×10^{12} Hz with a maximum deviation of 1.56×10^{13} Hz, which is 0.48% different from the linear value. The effective noise temperature has a standard deviation from the measured data of 0.57 K and a maximum deviation of 1.8 K or 1.1%. The diode output voltage has a standard deviation from the line of 9.90×10^{-7} V, and the maximum deviation is 4.08×10^{-6} V or 0.23% from the linear fit.

Due to the conversion loss of the mixer, the noise as defined at the receiver input varies more radically than (17) implies characterizing the amplifier alone. It would change by 4.7 K per kelvin of physical temperature change instead of 0.84 K per kelvin. This assumes a constant conversion loss of 7.5 dB and assumes the amplifier noise after down-conversion is the dominant added electronic noise. Both the noise and conversion loss of the mixer also vary with temperature. We noted that the conversion loss of the mixer did change when its temperature fluctuated. We also measured the ceramic filter. It is quite stable and changes by less than 0.04 dB over the entire passband for a 40-K temperature swing.

We performed all antenna temperature measurements while looking at a calibration load. The load we used was a piece of microwave absorber contained in an insulated box with a Styrofoam RF window. A thermocouple measured the absorber temperature, and fans circulated air about the absorber to minimize any temperature gradients [17]. We could vary the load temperature by heating the circulating air via a heating blanket over which the air flowed. One also could use cold loads or a known sky temperature to further the calibration range. The antenna always was pointed at the load during the test. Therefore, the radiometer output corresponded to a known antenna temperature.

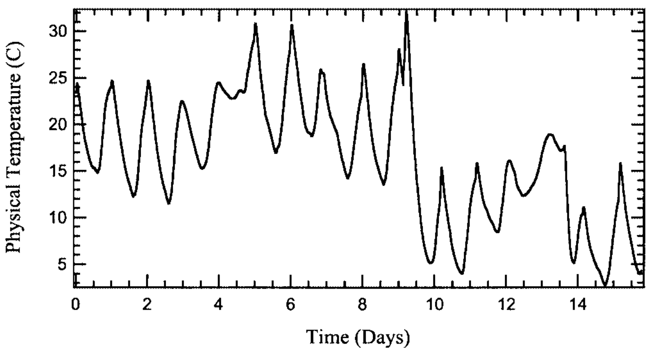

Fig. 2. Radiometer's physical temperature.

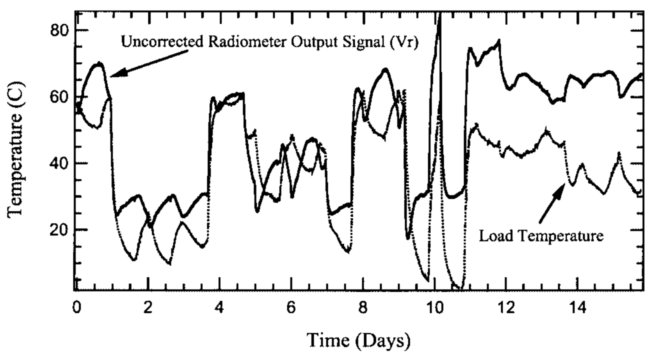

Fig. 3. Data with two-point calibration, but no temperature compensation.

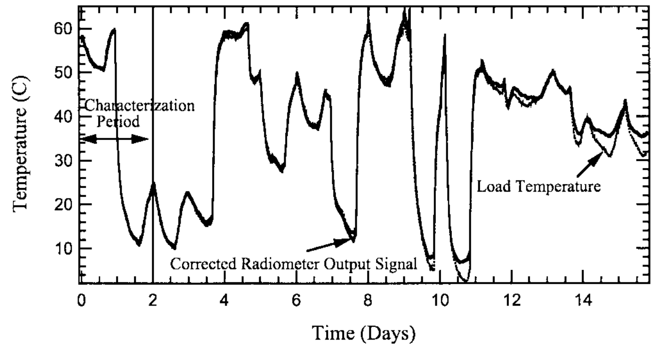

Fig. 4. Temperature-compensated radiometer output with the compensation calculated using a two-day characterization period.

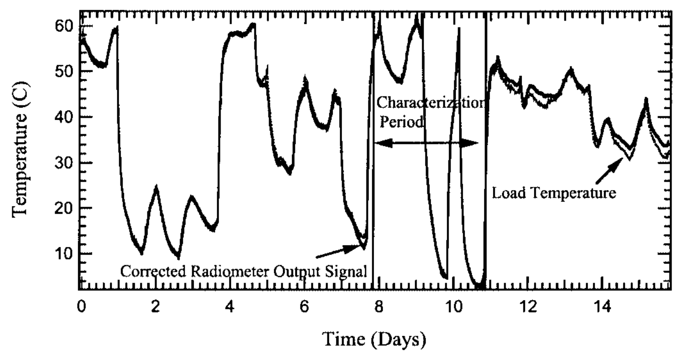

Fig. 5. Temperature-compensated radiometer output with a three-day characterization period that includes a larger physical temperature variation.

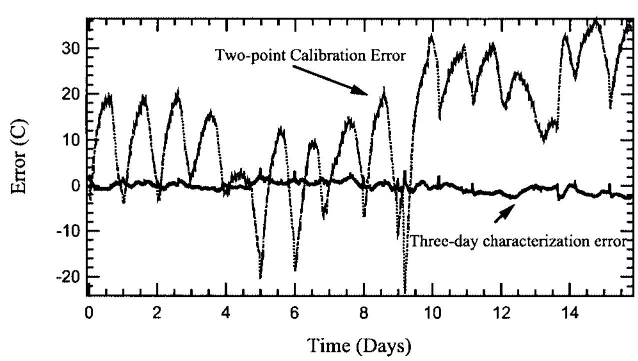

Fig. 6. Comparison of error between the data with a two-point calibration and the three-day characterization.

This arrangement allowed us to use any of the collected data for calibration and allowed us to calculate an error outside of the characterization period as the difference between the reading and load temperature.

V. Measured Results

Data was taken for 15 days between February 14–March 1, 2002, at the Applied Research Laboratories, The University of Texas in Austin. A cold front passed through Austin, TX, on the ninth day of taking data. Fig. 2 shows the physical temperature of the radiometer. For comparison purposes, a standard two-point calibration procedure was performed for a total power radiometer to obtain the calibration coefficients [18]. This method places two different temperature pieces of microwave absorber [19] T_{a1} and T_{a2} in front of the antenna and records the corresponding output voltage V_{r1} and V_{r2}. Using (4), the coefficients are

$$m_c = \frac{T_{a2} - T_{a1}}{V_{r2} - V_{r1}} \quad (19)$$

$$b_c = T_{a2} - m_c V_{r2}. \quad (20)$$

The antenna temperatures obtained from the two-point calibration (Fig. 3) do not follow the load temperature. In fact, the receiver variation with its physical temperature is so large that it forces the output signal up instead of down even though the load temperature is going down. The reverse is also apparent when the ambient temperature increases. The radiometer output has a peak-to-peak error of around 60 K. We performed the two-point calibration immediately before the data collection. The physical temperature of the radiometer was 23.3 °C, and the two load temperatures were 21.6 °C and 57.6 °C. The radiometer looked at each load for 30 s, the response was averaged over this period to get a better radiometric sensitivity, and (19) and (20) gave the calibration coefficients. m_{c0} was 141.58 *C/V*, and b_{c0} was −281.92 C.

By using the temperature correction with the first two days as a characterization period (Fig. 4), the peak-to-peak error decreases to 7.5 K with an average absolute error of 1.1 K. Since this period does not include the full range of the physical temperature swing, the characterization period shown in Fig. 5 that includes the full range gives better results. It has a peak-to-peak error of around 6.9 K and an average absolute error of 0.9 K. A comparison between the error using this characterization period and the uncompensated results is given in Fig. 6.

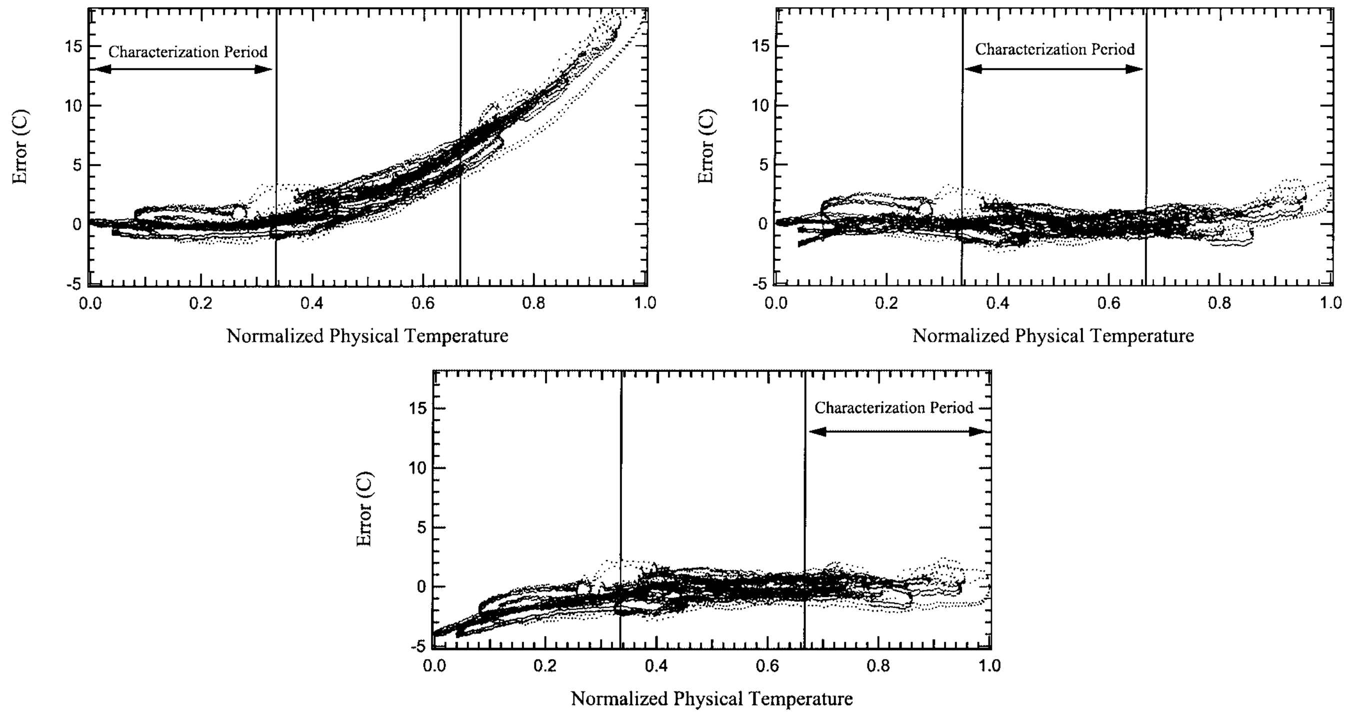

Fig. 7. Error for characterization periods including different ranges of the physical temperature of the radiometer.

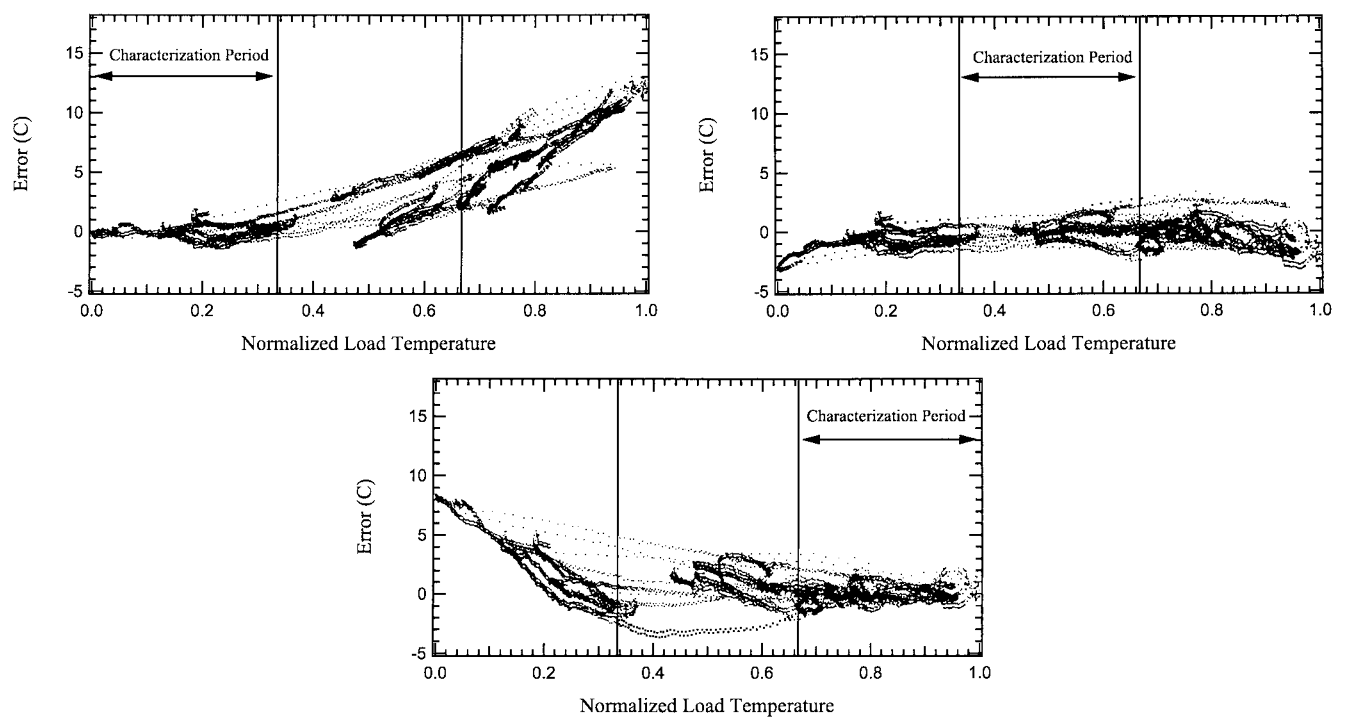

Fig. 8. Error for characterization periods including different ranges of the load temperature.

VI. Characterization Results

Errors start to increase when T_A and $T_{\rm phy}$ values begin exceeding the ranges used in the characterization. To see the effects the characterization ranges have on the error, we can order the data according to the physical or antenna temperatures. We can then calibrate over specific ranges in these temperatures and examine the error. Figs. 7 and 8 give the error when the characterization is performed for different thirds of the physical and load temperatures, respectively. The range used for characterization is indicated on the graphs. The error within any characterization period is less than 3.5 K. The characterization does not become immediately invalid as one moves away from the characterization range and stayed within 7 K in the ranges directly adjacent. However, the further one moves outside the range, the more the error increases.

VII. Discussion

This paper has shown a simple, inexpensive, and effective method of correcting output variations in total power radiometers due to changes in physical temperature. It has done so for a radiometer that allowed all of its components to change temperature over a wide range. It has addressed the handling of changes in system noise temperature due to physical temperature changes left out of previous studies using the temperature as a correction. This method provides a means to take advantage of the simplicity and sensitivity of the total power radiometer without the expense of the added microwave hardware of switched radiometers. Although it does not provide as precise of a measurement as switched radiometers, or temperature-controlled radiometers, it does provide a simple and inexpensive way to substantially reduce sensitivity of the output signal to changes in the physical temperature. The Dicke-switching requirement is absorbed into the microcontroller program, resulting in significant power and cost savings.

Possible improvements can be made in the current system. First, multiple temperature probes could be placed as near as possible to the temperature-sensitive components. This would be used in combination with a multivariable Taylor expansion of the calibration coefficients. Such a setup might decrease errors caused by a single probe not representing the temperature changes of all components. Second, the errors in physical temperature measurement caused by the probes and associated circuitry could be decreased. Third, all errors in the measurement of the load temperature could be minimized. Although the fans in the load were supposed to decrease the gradients in temperature across the microwave absorber, some could still exist. Further work is needed to determine the true limits of the temperature-compensation method.

References

[1] M. S. Hersman, “Sensitivity of the total power radiometer with periodic absolute calibration,” *IEEE Trans. Microwave Theory Tech.*, vol. MTT-29, pp. 32–40, Jan. 1981.

[2] R. H. Dicke, “The measurement of thermal radiation at microwave frequencies,” *Rev. Sci. Instrum.*, vol. 17, no. 7, pp. 268–275, July 1946.

[3] K. E. Machin, M. Ryle, and D. D. Vonberg, “The design of an equipment for measuring small radio-frequency noise powers,” *Proc. Inst. Elect. Eng.*, vol. 99, no. 59, pp. 127–134, May 1952.

[4] W. B. Goggins, “A microwave feedback radiometer,” *IEEE Trans. Aerosp. Electron. Syst.*, vol. AES-3, pp. 83–90, Jan. 1967.

[5] T. V. Seling, “The application of automatic gain control to microwave radiometers,” *IEEE Trans. Antennas Propagat.*, vol. AP-12, pp. 636–639, Sept. 1964.

[6] J. C. Greene, “Stability requirements and calibration of radiometers when measuring small noise powers,” *Proc. IRE*, vol. 45, pp. 359–360, Mar. 1957.

[7] F. D. Drake and H. I. Ewen, “A broad-band microwave source comparison radiometer for advanced research in radio astronomy,” *Proc. IRE*, vol. 46, pp. 53–60, Jan. 1958.

[8] J. S. Hey and V. A. Hughes, “A method of calibration centimetric radiometers using a standard noise source,” *Proc. IRE*, vol. 46, pp. 119–121, Jan. 1958.

[9] T. V. Seling, “An investigation of a feedback control system for stabilization of microwave radiometers,” *IRE Trans. Microwave Theory Tech.*, vol. MTT-10, pp. 209–213, May 1962.

[10] W. N. Hardy, K. W. Gray, and A. W. Love, “An S-band radiometer design with high absolute precision,” *IEEE Trans. Microwave Theory Tech.*, vol. MTT-22, pp. 382–390, Apr. 1974.

[11] E. A. Ohm and W. W. Snell, “A radiometer for a space communications receiver,” *Bell Syst. Tech. J.*, vol. XLII, no. 5, pp. 2047–2080, Sept. 1963.

[12] J. P. Hach, “Proposal for a continuously calibrated radiometer,” *Proc. IEEE*, vol. 54, pp. 2015–2016, Dec. 1966.

[13] ——, “A very sensitive airborne microwave radiometer using two reference temperatures,” *IEEE Trans. Microwave Theory Tech.*, vol. MTT-16, pp. 629–636, Sept. 1968.

[14] N. Skou, *Microwave Radiometer Systems: Designs and Analysis*. Norwood, MA: Artech House, 1989.

[15] K. Al-Ansari, P. Garcia, J. M. Riera, A. Benarroch, D. Fernandez, and L. Fernandez, “Calibration procedure of a microwave total-power radiometer,” *IEEE Microwave Wireless Comp. Lett.*, vol. 12, pp. 93–95, Mar. 2002.

[16] D. A. Thompson, “Pilot signal correction and physical temperature compensation of drift in total power radiometers,” Ph.D. dissertation, Dept. Elect. Comput. Eng., Univ. Texas at Austin, Austin, TX, 2002.

[17] C. D. Govan, “A wide-band frequency tunable Dicke radiometer and microwave radiometric measurements,” Appl. Res. Labs., Univ. Texas at Austin, Austin, TX, TD 04A1003, 1995.

[18] F. T. Ulaby, R. K. Moore, and A. K. Fung, *Microwave Remote Sensing: Active and Passive*. Reading, MA: Addison-Wesley, 1981, vol. 1.

[19] W. N. Hardy, “Precision temperature reference for microwave radiometry,” *IEEE Trans. Microwave Theory Tech.*, vol. MTT-21, pp. 149–150, Mar. 1973.

David A. Thompson, photograph and biography not available at time of publication.

Robert L. Rogers (M’98–SM’99) was born in San Angelo, TX, in 1961. He received the B.S., M.S.E., and Ph.D. degrees from The University of Texas at Austin, in 1983, 1985, and 1989, respectively, all in electrical engineering.

Upon graduation, he joined the Applied Research Laboratories, The University of Texas at Austin, where he is currently a Principal Investigator. He has been involved in the areas of microwave and millimeter-wave antennas, electrically small antennas, radar, radiometry, communications systems, and high-power pulsed energy systems. His research interests are in the areas of remote sensing, communications, wireless networking, and antennas.

John H. Davis (S’67–M’67) received the Ph.D. degree from The University of Texas at Austin.

He is currently an Associate Professor with The University of Texas at Austin. He is interested in the areas of mixed signals, radiometry, RF, and microwave devices and holographic antenna measurements.